Secondary Flows in Axial Turbines – A Review

L.S. LANGSTON

University of Connecticut
Mechanical Engineering Department
191 Auditorium Road, U-3139
Storrs, CT 06269 USA

ABSTRACT: An important problem that arises in the design and the performance of axial flow turbines is the understanding, analysis, prediction and control of secondary flows. Sieverding[1] has given a review of secondary flow literature, covering up to 1985. In this paper a brief review of pre-1985 work is given, and then a survey of open literature secondary flow investigations since the Sieverding review is presented. Most of the studies reviewed deal with plane or annular cascade flows. Tip clearance effects are not covered. The basic secondary flow picture for a turbine cascade, as measured and verified by a number of investigators is described. Recent work that shows refined secondary flow vortex structures is examined. A flow parameter based on inlet boundary layer properties used to predict horseshoe vortex swirl is presented. Work on secondary flow loss reduction, involving airfoil geometry, endwall fences and endwall contouring is briefly reviewed. A new leading edge bulb geometry that has demonstrated impressive loss reduction is considered. It is concluded that accurate routine prediction of secondary flow losses has not yet been achieved, and must await either a better turbulence model or more experiments to reveal new endwall loss production mechanisms. Lastly, loss is examined from the standpoint of entropy generation.

INTRODUCTION

Bradshaw[2] has aphoristically observed: "Of all the fluid-dynamic devices invented by the human race, axial-flow turbomachines are probably the most complicated." One important contributor to this complexity is the fluid flow and heat transfer brought about by the existence of endwalls in axial flow turbomachine gas path passages. Due to viscous effects, endwalls divert primary flow produced by blades and vanes, to give rise to what has come to be called secondary flow, or endwall flow.

The secondary or endwall flow in a cascade of turbine blades or vanes (such as depicted in Fig. 1) constitutes one of the most commonplace and widespread three-dimensional flows that arise in the generation of electrical and motive power. Such fluid flows occur in all axial flow turbines (gas, steam and water) used to generate most of the world's electricity. They occur in all of the jet and turboprop engines (30,000 in the inventory (1993) of the U.S. Air Force, alone) which power most of the aircraft of the world.

By turbine designer conventions, the effects of the highly interactive flow picture in Fig. 1 is artificially broken down to those caused by the blade or vane "profile" surface and those caused by the endwall. (A third category of tip clearance effects will not be treated in this paper.) The aerodynamic losses so attributed to the endwall – usually termed secondary flow losses or secondary losses – can be as high as 30-50% of the total aerodynamic losses in a blade or stator row, according to Sharma and Butler[3]. Inlet guide vanes, with lower total turning and higher convergence ratios, will have smaller secondary losses, amounting to as much as 20% of total loss for an inlet stator row.

Because of the essential importance of secondary flow in all kinds of power turbines, research in the last 25 years has been quite extensive. Sieverding[1] has reviewed secondary flow literature up to 1985. The goal in this paper is to build upon this excellent 1985 review and to examine some of the secondary flow research since its publication. Text length considerations here allow for either a shallow listing of a large number of secondary flow studies, or a focus on a smaller number. The author has chosen the latter path (the focus) and asks the indulgence of those precluded.

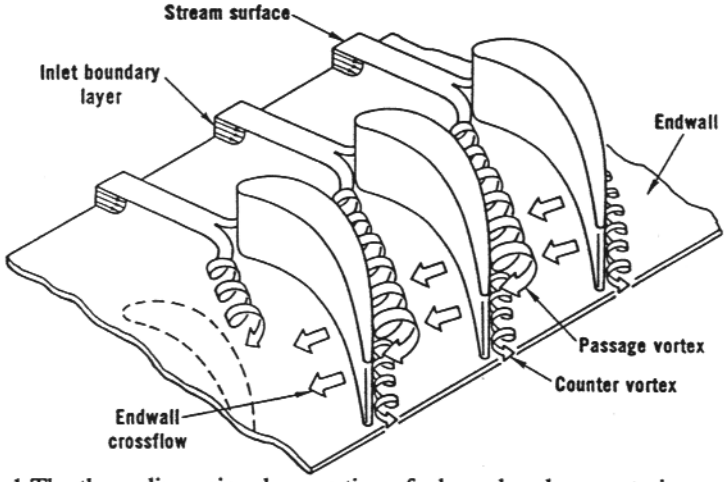

Fig. 1 The three-dimensional separation of a boundary layer entering a turbine cascade. The saddle point occurs where the vortex is formed.

THE BASIC FLOW PICTURE

The hardware sketched in Fig. 1 represents a plane (or linear) cascade, depicting the airfoils and endwalls in a turbomachine with a very large (infinite) radius. For many years now, experimenters studying these intriguing, but complex three-dimensional flows in axial turbines, have made use of planar cascades to sort out and measure fluid flow and heat transfer features. Numerical calculators modeling these flows have also relied on simple plane cascade geometries to attempt to "postdict" existing cascade data, or to separate out the effect of various analytical techniques (such as turbulence models).

The basic flow through a plane turbine cascade has been fairly well studied, documented and verified by many experimenters (See Sieverding[1]). One of the earliest complete studies was done by Langston, Nice and Hooper[4] who used a very large scale, low aspect ratio plane cascade of four turbine airfoils. In their work, detailed measurements of subsonic flow were made at axial planes upstream, within and downstream of the plane cascade.

The three-dimensional flow they measured is that shown schematically in Fig. 1. This figure, taken from Langston[5], shows that at the endwall of the cascade, the inlet boundary layer separates at a saddle point and forms a horseshoe vortex. One leg of this vortex (sometimes called the "pressure" leg), drawn into a cascade passage, is "fed" by the passage pressure-to-suction endwall flow and becomes the passage vortex. The other leg (called the "suction" leg) is drawn into an adjacent passage and has an opposite sense of rotation to the larger passage vortex. This smaller vortex is labeled as a counter vortex in Fig. 1 and can be thought of as a "planet" possibly rotating about the axis of the passage vortex (the "sun"). Thus the position of the counter vortex relative to the passage vortex may be different than that shown in Fig. 1. The ribbon arrows in the figure have been drawn to exaggerate vortex motion. The actual rotation of the vortices is much less than shown (about two rotations for the passage vortex).

Sieverding and Van den Bosche[6] showed the development and interaction of the passage and counter vortices by marking with smoke, two stream surfaces initially parallel to an endwall in low speed air flow entering a cascade. As shown in the sketch of their results in Fig. 2, one can see the evolution and movement of each vortex (as evidence by stream surface curling), using the planet and sun analogy of the last paragraph.

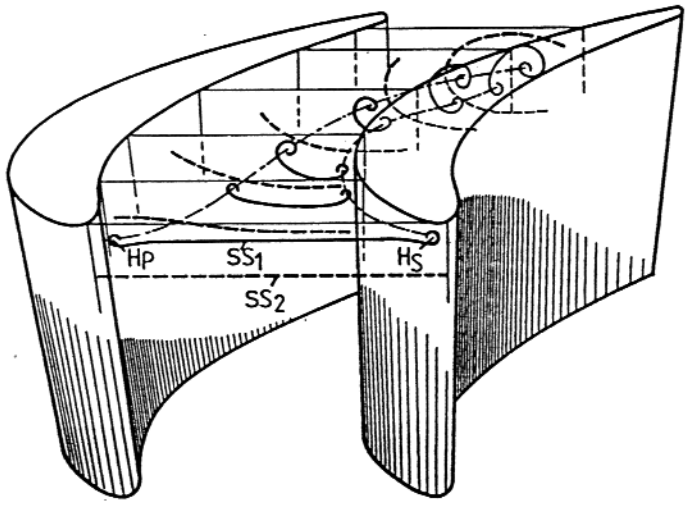

Fig. 2 Laminar flow stream surfaces SS_1 (within inlet boundary layer) and SS_2, from Sieverding and Van den Bosche[6], where H_p – pressure side horseshoe vortex leg, and H_s – suction side horseshoe vortex leg.

From the important standpoint of the turbine designer, this endwall vortex secondary flow is responsible for a loss of lift (i.e. loss of turbine work) and an increase in aerodynamic loss (i.e. a decrease in turbine efficiency), when compared to a hypothetical two-dimensional cascade flow.

The loss in lift is shown by static pressure data plotted in Fig. 3, from Langston, Nice and Hooper[4]. Values of the static pressure coefficient, c_p, taken with pressure taps mounted on the suction and pressure airfoil surfaces at 2.3, 12.15, 25 and 50 percent of span (measured from one endwall) are shown in Fig. 3, as a function of nondimensional axial distance, x. The two curves plotted in Fig. 3, the result of a two-dimensional incompressible potential flow calculation, are shown for purposes of comparison.

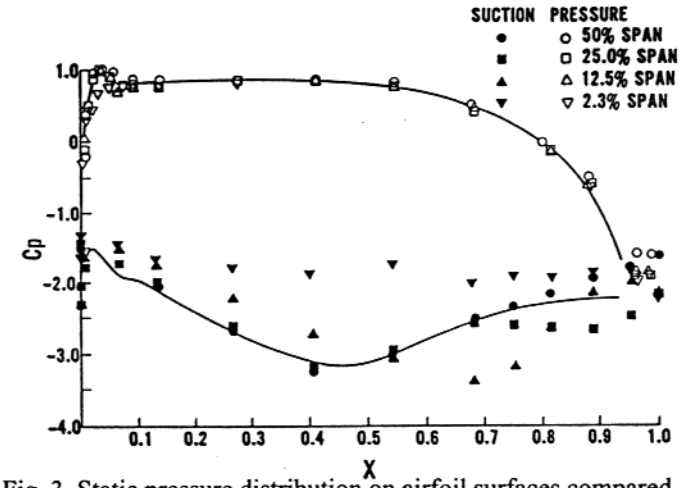

Fig. 3 Static pressure distribution on airfoil surfaces compared with potential flow (Langston[4]).

The pressure-side data shows two-dimensional behavior for all spanwise locations. On the suction-side, the data at midpsan (50 percent) exhibits two-dimensional behavior, except near the trailing edge, where viscous effects (trailing edge separation) influence the flow. As discussed in more detail in Langston[4] the suction-side pressures at other spanwise locations (25, 12.5 and 2.3 percent) show the effect of the passage vortex formed on the endwall of the cascade. The net effect of this three-dimensional "secondary flow" is to decrease the area between the suction and pressure side pressure distribution data points, for a given spanwise position. This area is a measure of the net lift (work output), so that the Fig. 3 data clearly shows a decrease of lift on the airfoil, as the endwall is approached from midspan.

The growth of mass-averaged aerodynamic loss coefficient, c_{pt}, a function as nondimensional axial distance x through the cascade is shown in Fig. 4, taken from Langston[4]. Also shown is the measured mass coefficient, η, (the inverted triangular data points) which show that mass was conserved (i.e. all values are close to $\eta = 1$). The measured mass-averaged loss values in Fig. 4 show that near the inlet of the cascade there is only a slight increase in loss as the inlet boundary layer (the value near $x = -0.2$) becomes the horseshoe vortex (up to about $x = 0.3$). Then, beyond a value of $x = 0.5$, the mass-average loss values rise rapidly as the passage vortex dramatically increases in size in the region of decelerated suction-side flow ("uncovered" turning, where the pressure rises rapidly in the downstream direction). Then, as the flow leaves the cascade ($x > 1.0$) the mass-averaged loss values rise rapidly again as passage vortex flow and the skewed endwall boundary layer are mixed-out and turned to a nominal exit flow angle, by the mainstream flow.

SECONDARY FLOW RESEARCH SINCE 1985

The basic secondary flow picture described in the last section was arrived at from examination of detailed velocity, pressure, and flow visualization measurements made upstream, within and downstream of turbine cascade flow passages. Pre-1985 investigations were reported by Langston, Nice and Hooper[4], and Marchal and Sieverding[7]. Post-1985 works that report on complete flow field measurements include

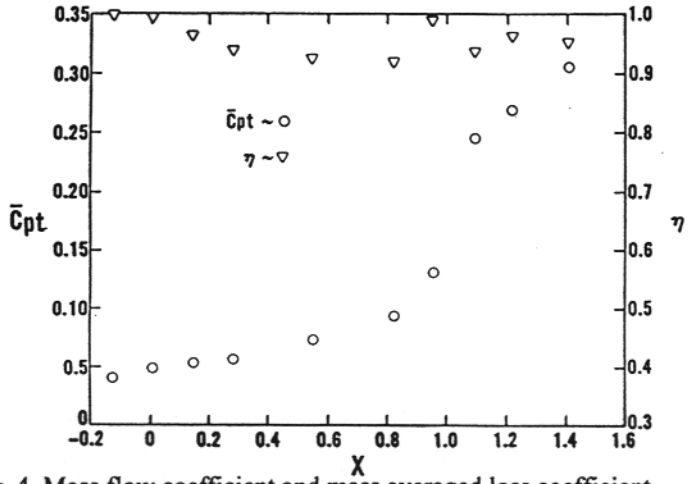

Fig. 4 Mass flow coefficient and mass averaged loss coefficient as a function of axial distance through the cascade (Langston[4]).

Yamamoto[8,9], Gregory-Smith, Graves and Walsh[10], and Harrison[11]. One can now build upon this firm foundation of endwall flow physics to examine some of the secondary flow research that has gone on since Sieverding's[1] 1985 review.

Other Endwall Vortex Flow Patterns

Sharma and Butler[3] proposed a slightly different version of the vortex pattern of Fig. 1. Their modified flow pattern is shown in Fig. 5, with the counter vortex wrapping around the passage vortex. (This wrapping wasn't evident in the velocity and pressure flow field measurements of Langston[4].) They deduced the flow pattern of Fig. 5 from the work of others and their own experimental observations. They used this approach to formulate a semi-empirical model for estimating losses in a turbine. Secondary flow loss correlations based on experimental data have long been a basic design tool, especially in the early design stages of any new axial flow turbine. Usually, it is not until later in the design cycle that CFD (computational fluid dynamics) codes are used (and then, sometimes with limited success in predicting losses, as will be discussed later). One of their key findings was that inlet boundary layer losses are convected through the cascade without causing any additional losses, and is independent (counter to classical secondary flow theory) of the amount of turning. In effect, the saddle point separation of the inlet boundary layer decouples it from the downstream effects of turning.

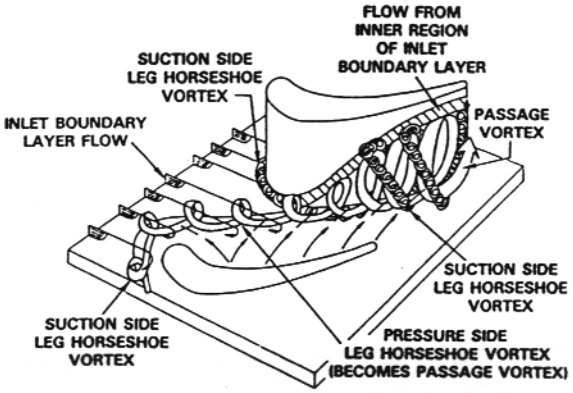

Fig. 5 Endwall vortex picture of Sharma and Butler[3].

Another endwall vortex pattern revision to Fig. 1 has been put forth by Goldstein and Spores[12] of the University of Minnesota. The Minnesota group has a long history of reporting detailed mass transfer measurements (naphthalene sublimating into wind tunnel air) to infer heat transfer coefficient distributions on endwalls and airfoils in a cascade. Their measurements of mass transfer show a very high concentrated mass transfer rate (5 times flat plate values) right at the leading edge-endwall junction of their high pressure turbine blades, at a Reynolds number in the range of engine operating conditions. This led them to postulate the existence of another very small and intense vortex at the junction, which Goldstein and Spores called a leading edge vortex.

In a later, very detailed flow visualization study of a similar cascade flow, Wang, Olson, Goldstein and Eckert[13] documented the endwall flow using laser light and multiple smoke wires (similar to Sieverding and Van den Bosche[6]). Their multivortex flow pattern is shown in Fig. 6. Because they ran at a low Reynolds number (for flow visualization with smoke) some of the features they found seem to be similar to the complex periodically varying horseshoe vortex pattern formed in front of an endwall mounted cylinder in laminar flow (e.g. see Baker[14]).

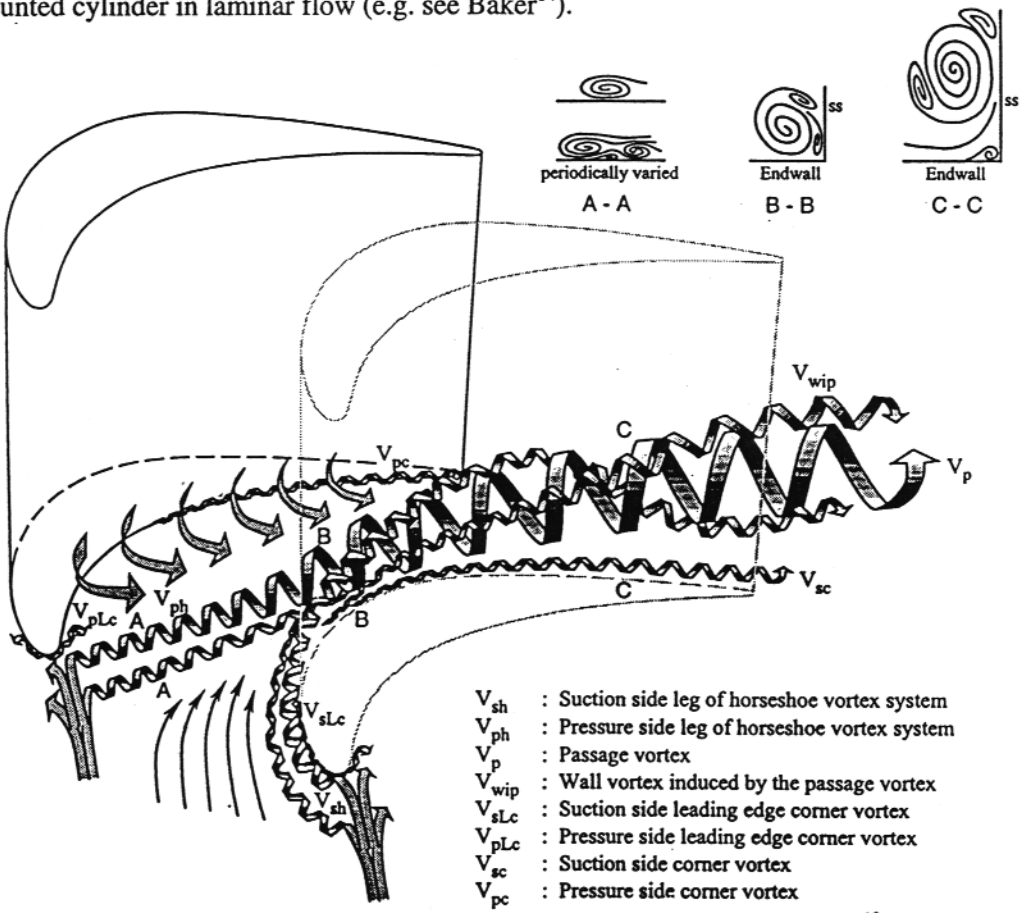

Fig. 6 Endwall Vortex Picture of Wang, Olson, Goldstein and Eckert[13].

The modifications to the secondary flow in Fig. 1 proposed by Sharma[3] (Fig. 5) and by Goldstein and Spores[12] and Wang, et al[13] (Fig. 6) add to the complexity of the vortex picture. Further work is necessary to verify that these inferred modifications exist, through the use of flow field measurements of pressures, velocities and vorticity. A good

example of such verification was the low-pressure turbine cascade study by Hodson and Dominy[15]. However, their attempt to make a complete endwall vortex tracing was hampered somewhat by the relative small size of their cascade relative to the size of their instrumentation.

As Green[16] points out, "vortex" is an inherently fuzzy term. He offers the definition of a vortex ".....as the feature of a flow field that a majority of fluid dynamicists would label as such." This definition is not of much help to a turbine designer who might be trying to account for the effects of secondary flows on endwall heat transfer or aerodynamic losses. Other definitions are based on concentrated or distributed vorticity, and on circulation. For turbine design purposes the author defines a vortex as a flow feature in the turbine gas path, composed of a collection of throughflow streamlines spiraling around a center of low static pressure to produce simple closed curve isobars (of static pressure) in successive planes normal to the throughflow. (An example is shown in Figs. 8 and 9 of Langston[4] and in Figs. 6 and 9 of Eckerle and Langston[17].)

Inlet Boundary Layer Separation

Some progress has been made on understanding the flow conditions that occur when the inlet endwall boundary layer separates at the saddle point on the endwall and rolls up into the horseshoe vortex (see Figs. 1, 5 and 6). Thus far there is no quantitative criterion for determining the saddle point location. Data presented by Langston[4] shows that its location occurs in a region of stream wise adverse pressure gradient, and that it is most strongly dependent on the incidence angle of the cascade flow. The work of Moore and Ransmayer[18] which is reviewed in Sieverding[1], involved the modification of a cascade blade cylindrical leading edge with a sharper, wedge-shaped extension of the leading edge. Moore and Ransmayer saw no change in their airfoil pressure distribution and no appreciable change in endwall loss production, with the addition of the sharp leading edge to the cascade airfoils. They assumed they had eliminated the horseshoe vortex with the sharp leading edge, and, since they saw no change in exit loss, concluded the horseshoe vortex has little effect on loss. However the author draws the opposite conclusion from their results; that is, their sharp leading edge had no effect on the formation of the horseshoe vortex, and it was <u>not</u> eliminated in their tests. The separation at the saddle point is not dependent on the radius of curvature of the airfoil edge, but is dependent on the pressure field generated by the overall shape and size of the pressure and suction surfaces of the airfoils. The axial chord of the airfoil would be the significant length since it would characterize the airfoil pressure field, rather than a leading edge radius.

The symmetrical separation of boundary layer flow normal to a circular cylinder mounted on an endwall is perhaps the simplest of geometries that demonstrate a horseshoe vortex system where the cylinder diameter is the important dimension. One such study was carried out by Eckerle and Langston[17]. They provided a detailed description of the vortex system around the base of a single cylinder mounted in a wind tunnel. The side walls of the tunnel acted as planes of symmetry so that their actual single cylinder was one element of a cascade of cylinders at zero incidence angle. The Eckerle-Langston single cylinder experiment yielded a symmetrical saddle point (asymmetric for a turbine cascade) whose position occurred in a region of an adverse pressure gradient (as in the turbine cascade), upstream of the cylinder. Recently, research

on the characteristics of horseshoe vortices has been extensively reviewed by Ballio, Bettoni and Franzetti[19].

Eckerle and Awad[20] carried out more detailed studies of the horseshoe vortex formation in front of a cylinder and varied the free stream velocity, making extensive velocity measurements with a laser doppler anemometer system. Their most important finding was that they could correlate their data and the data of others with the nondimensional parameter E, where

$$E = (\mathrm{Re}_D)^{\frac{1}{3}} \left(\frac{D}{\delta^*} \right) \qquad (1)$$

Re_D is the cylinder Reynolds number, D is the cylinder diameter and δ^* is the displacement thickness of the boundary layer at the position of the leading edge of the cylinder (without the cylinder).

Their results showed that for E > 1000, no swirling motion was present in the plane of symmetry upstream of the cylinder. The vortex motion of the separating boundary layer developed at an angular distance from the plane of symmetry. For E < 1000 the swirling motion of the vortex was initiated in the plane of symmetry. As the authors point out, the identification of these two regimes gives a turbine designer a better way to predict effects of the separating flow on the heat transfer and effectiveness of a coolant film in the saddle point region of the endwall. The Eckerle-Awad parameter given by Equ. (1) allows one to predict saddle point flow behavior in a turbine. Because of endwall clearance gaps between blade and stator rows in a turbine one can argue that certainly there are instances when the upstream developing endwall boundary layer is very small. This would make E large, and if its value is greater than 1000 as given by Equ. (1), the turbine heat transfer designer can expect the gas path flow in the region of the saddle point to be swirl-free.

Recently, Kang, Kohli and Thole[21] measured heat transfer and the flow field in the leading edge region of a first stage stator cascade, at two Reynolds numbers of 6×10^5 and 1.2×10^6, based on inlet velocity and stator true chord. Fig. 7 shows the inplane velocity vectors for the two Reynolds numbers they measured in what they term a stagnation plane. This is a plane extending radially outward from the stator leading edge and passing through the saddle point. For their smaller Reynolds number case (0.6×10^6) the value of the Eckerle-Awad parameter was E=990 (based on stator axial chord). As can be seen in Fig. 7, the inplane velocity vectors do show a swirling flow as the horseshoe vortex forms, in agreement with the Eckerle-Awad limit. For the larger Reynolds number case (1.2×10^6) E=1640, and the velocity vectors in Fig. 7 exhibit no swirl, for E>1000.

Thus the parameter E and the Eckerle-Awad limit of 1000 seem to accurately characterize turbine cascade saddle point flow on the endwall for swirl or no-swirl, if axial chord is used as an effective cylinder diameter. Certainly more work needs to be done to validate this conclusion, but Equ. (1) holds the promise of providing one of the first parameters to quantify the flow resulting from the separation of a turbine cascade inlet boundary layer.

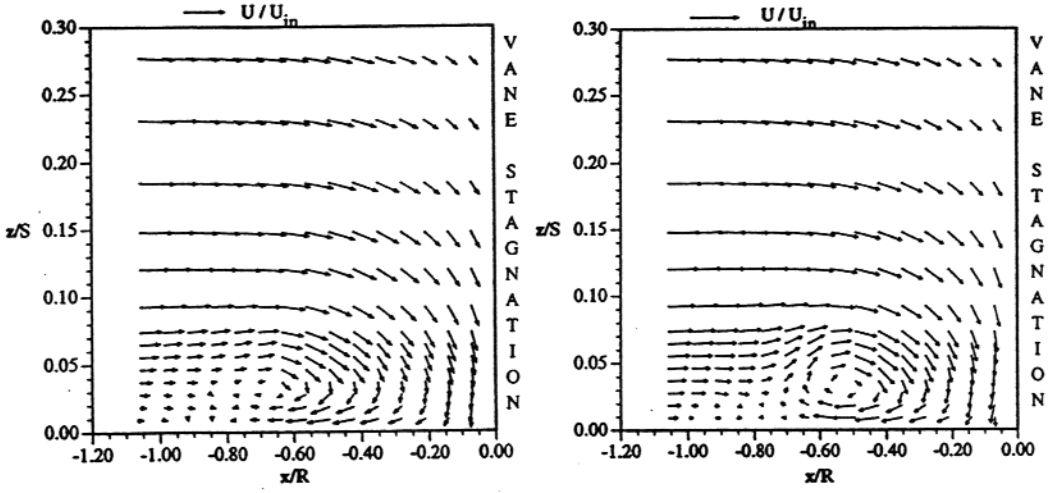

Fig. 7 Kang et al[26] mean velocity vectors on stagnation plane.
On the left: E=1640, Re = $1.2X10^6$. On the right: E=990, Re = $0.6X10^6$.

Secondary Flow Loss Reduction

Because secondary or endwall losses can be so high (30-50% of total loss, as stated earlier) there have been many attempts and studies to reduce them. Various "bowed" and "leaned" airfoils have been experimented with and are in use on many newer jet engines designs, to manage endwall and profile losses. As far as the author is aware, there have been no dramatic loss reductions by either the use of bowing or leaning. Harrison[22] presents a systematic study of both, and more recently Duden, Raab and Fottner[23] show the results of an experimental and design program for three-dimensional cascade airfoils and endwall contouring.

The use of fences and grooves on endwall and suction side airfoil surfaces was extensively investigated by Prumper[24] to reduce secondary flow losses. Prumper tested upwards of 400 different inlet guide vane configurations on a low aspect ratio annular cascade. His optimum configuration involving shallow grooves cut on the suction side vane surface at the endwall, improved the efficiency (by one percentage point) and off-design performance of an existing commercial single stage turbine (see Gallus and Kummel[25]). More recent studies on endwall fences have been carried out by Chung and Simon[26] and Aunapu, et al[27].

Endwall contouring, especially in inlet guide vane passages, has been a major focus for many years. Among the first to test an "S" shaped endwall was Deich, et al[28] who were able in increase the efficiency of an existing turbine by profiling the hub endwall of turbine inlet guide vanes into a sigmoidally curved surface converging in the streamwise direction. Later, Morris and Hoare[29] did detailed planar cascade S-wall studies, showing that endwall losses were significantly reduced at the non-contoured endwall. Kopper and Milano[30] carried out S-wall testing on inlet guide vanes in linear

cascades and measured a 17% reduction of full passage mass-averaged loss relative to a full planar endwall configuration. More recent studies involving testing and CFD calculation on S-walls by Dossena, Perdichizzi and Savini[31] yielded results similar to Kopper and Milano[30].

Preliminary research on one unusual, but promising approach to endwall contouring has been reported by LaFleur, Whitten and Araujo[32]. This technique makes use of the shape of ice that has been formed on the refrigerated endwalls of turbine cascade passages, as water is run through them. Where water circulation or wall shear forces are low ice grew in thickness, and where either was high, less ice formed. By applying this technique to a cylinder mounted on an endwall, LaFleur and Langston[33] were able to show through wind tunnel testing that the total drag (or aerodynamic loss) for the ice-shaped endwall surface was reduced by 18% when compared to smooth, non-contoured endwall and cylinder combination.

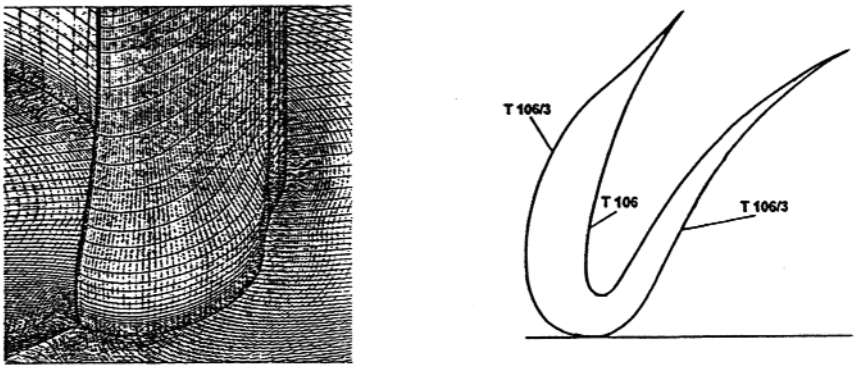

Fig. 8 Turbine endwall modification by Sauer, Müller and Vogeler[34]. The leading endwall bulb (T106/3) reduced endwall losses (of T.106) by 47%.

One of the most promising results on reducing secondary flow losses by contouring has been presented by Sauer, Muller and Vogeler[34]. They positioned a leading edge "bulb" at the endwall-airfoil junction of high turning turbine airfoils in a plane cascade. Their bulb geometry (presumably analogous to the bulb on a ship's prow used to reduce bow wave drag) fairs into the leading edge in a spanwise direction and has its largest thickness at the suction side-endwall junction, as shown in Fig. 8. The authors report an experimentally determined 47% reduction in net secondary loss using the bulb in a low pressure turbine airfoil cascade with an aspect ratio of 3.0 at a Reynolds number of 4×10^5. In an earlier work using similar bulb geometry lower turning, inlet guide vane-like turbine cascades, Sauer and Wolf[35] reported reductions of net endwall loss of up to 25%. Sauer, et al[34,35] reason that these remarkable reductions in loss are brought about by the bulb increasing the strength of the counter vortex (see Fig. 1), which reduces the strength of the passage vortex with its opposite sense of rotation. But one can also argue that such a proposed mechanism would actually increase losses, as measured downstream of the cascade trailing edge plane. (Sauer, et al[34] were unable to provide answers through the use of a CFD model.) Clearly some experiments involving endwall measurements within cascade passages are needed to give more information on how these leading edge bulbs give such promising secondary loss reductions.

Secondary Flow Prediction

There are no closed form analytical solutions to the secondary flow shown in Fig. 1. Since the early 1970's there has been a great deal of effort to model this complex flow using a variety of CFD codes and associated turbulence models. Only a few representative examples will be briefly examined here, of the many reported in the open literature. Much progress has been made and it would be safe to say that most turbine manufacturers use 3-D CFD codes routinely in the mid to later stages of the design process for a new machine. Generally loading curves (i.e. airfoil pressure distributions as shown in Fig. 3) can be predicted accurately even when secondary effects are quite large. However, the ability to *routinely* predict aerodynamic losses with strong secondary flows (e.g. Fig. 4) has been more limited.

Hah[36] in 1983 was one of the first investigators to develop a numerical code that captured most of the secondary flow features (Fig. 1). Comparing his calculations with the data of Langston, Nice and Hooper[4], he used a modified algebraic Reynolds stress model for the turbulence closure problem. An examination of his results show very good agreement with static pressure data on the airfoil (Fig. 3) and fairly good agreement with the endwall static pressure distributions. His calculations of aerodynamic loss through the cascade passage showed the overall trends of the data in Fig. 4 (e.g. the slow growth of loss in the first part of the passage and then the sudden jump near the trailing edge), but the calculated mass averaged loss coefficients, c_{pt}, were 20-30% higher near to and downstream of the trailing edge.

Nearly 10 years later, Dorney and Davis[37] calculated fluid flow and heat transfer for the Langston et al[4] cascade, using the thin inlet boundary layer heat transfer and aerodynamic data of Graziani, Blair, Taylor and Mayle[38], with much better accuracy. The authors' results using a Baldwin-Lomax two-layer algebraic turbulence model show excellent agreement for static pressures on airfoil surfaces and the endwall when compared to data. A grid refinement study was done, and for their finest grid, they predicted the measured overall area-averaged loss just downstream of the cascade within 2%. (It should be noted that the experimental loss values were not given in the original Graziani et al[38] paper.) The Dorney and Davis work is not representative of typical CFD design simulations used for engine design. They used a CRAY-2 supercomputer and their computational times were relatively large. They used very fine grids (up to 900,000 grid points for full span) whose construction was influenced by knowledge of existing heat transfer and fluid flow experimental data.

The recent work of Hartland, Gregory-Smith and Rose[39] might be more typical of CFD calculations used in a turbine design system. They report on mass averaged total pressure loss measurements made in the large scale turbine cascade of Gregory-Smith and Cleak[40]. Their measurements were made first in a planar endwall cascade and then in a non-axisymmetric endwall cascade, contoured to reduce the strength of the passage vortex. The net mass-averaged total pressure loss, c_{pt}, for each of their configurations was calculated using a Rolls-Royce standard turbomachinery CFD code, described by Harvey, et al[41]. Their net mass-averaged losses across the cascade, measured and predicted, are given in Table 1.

From the values given in Table 1, it can be seen that the CFD code over-predicted full losses by as much as 75%, overpredicted mid-span losses by as much as

173% and underpredicted the secondary losses by as much as 47%. Also, the CFD calculations predicted the planar endwall to be the smaller loss producer, whereas the experimental values showed just the opposite, with a reduction in "full" loss of 20% provided by the contoured endwall. Thus the CFD results were not correct either from a quantitative or a qualitative standpoint. Hartland et al[39] attribute this limited success in loss prediction to the lack of an adequate turbulence model. The authors' state: "The CFD predicts the secondary kinetic energy well, but the mixing length turbulence model is not adequate to translate this into accurate losses. The modelling required to improve on this is not clear, however. Moore and Gregory-Smith[42] found that for the code used in this design, a k-ε turbulence model performed rather worse than a mixing length model, especially if laminar and transitional regions are allowed for in the latter. More work in this area is needed."

Table 1. Net losses, c_{pt}, for the Durham cascade as given in Table 3 of Hartland, Gregory-Smith and Rose[39].

Endwall Configuration Measured/CFD	c_{pt}		
	Full	Mid-Span	Secondary
Contoured	0.1108	0.0557	0.0551
Planar	0.1377	0.0598	0.0780
CFD Contoured	0.1937	0.1518	0.0419
CFD Planar	0.1926	0.1512	0.0414

Bradshaw[2] has observed that turbulence modeling for complex flow (e.g. turbomachinery) represents an "unfinished business". He further concludes: "The present state is that even the most sophisticated turbulence models are based on brutal simplifications of the N-S equations and cannot be relied on to predict a large range of flows accurately. For example – a particular embarrassment to the modeling community – a model that is adjusted empirically to give good results for plane jets from "two-dimensional" nozzles often gives poor results for jets from circular nozzles."

In addition to the possible shortcomings of turbulence modeling, the author is of the opinion that at least one loss producing mechanisms may not be being modeled correctly, namely the highly skewed boundary layer on the endwall. This boundary layer is very thin and much of it is laminar as seen early on by Senoo[43] and Langston[4], and later by Harrison[11,22]. Strongly accelerated laminar flows (e.g. Falkner-Skan flows) can give local friction coefficient and heat transfer coefficient values many times greater than nonaccelerated cases. Skewing such flows (as occurs on an endwall) further increases heat transfer and wall shear forces from collateral boundary layer values. More experimental work is needed to correctly model the laminar portion of the endwall boundary layer.

Secondary Flow Loss Reconsidered

Thus far in this paper secondary flow "loss" has been treated without regard to a rigorous definition, rather in the same way that Oliver Heaviside, the English physicist, defended some of his important (but unproven) mathematical results: "Shall I refuse my dinner because I do not fully understand the process of digestion?"

A clear and simple explanation and example of aerodynamic loss – or simply, loss – has been given by Taylor[44]. Consider the adiabatic flow of an ideal gas through a stationary screen or vane row. If the upstream (station 1) and downstream (station 2) flow is steady and uniform, the thermodynamic state can be completely specified by the stagnation temperature, T_0, and the stagnation pressure, P_0, at each station. Since no work is done and no heat is transferred, $T_{01} = T_{02} = T_0$, but due to the friction forces caused by the interaction of the gas and the screen (or vanes), the stagnation pressure, P_o, will change. Taylor shows that the specific work, w, that would be required to restore the fluid (the ideal gas) to its initial (station 1) state would be

$$w = \frac{1}{\rho_{01}} \left(P_{01} - P_{02} \right) \tag{2}$$

where ρ_{01} is the upstream stagnation density and $P_{01} - P_{02}$ is the change in total or stagnation pressure. From this idealized example one can see that what is "lost" in the irreversible frictional flow through the screen or vanes is the ability to do work, as given by Equ. (2), and that the change in stagnation or total pressure ($P_{01} - P_{02}$) is a direct measure of the lost work. This pressure difference can be nondimensionalized with the station 1 velocity head to form the basis of the mass-averaged total pressure loss coefficient, c_{pt}, used in Fig. 4 and in Table 1. Following Taylor[44], Equ. (2) can be rewritten as

$$s_2 - s_1 = \frac{R}{P_{01}} \left(P_{01} - P_{02} \right) \tag{3}$$

where R is the ideal gas constant and $s_2 - s_1$ is the entropy increase in the fluid after it has passed through the screen or vane row. Thus the change in total pressure is also a direct measure of entropy generation.

Denton[45], in the 1993 IGTI Scholar Lecture, has proposed that the understanding of loss in turbomachines will be improved by thinking of it in terms of entropy generation, such as given by the simple example that resulted in Equ. (3). In this insightful paper he treats some of the sources of entropy that cause loss, such as viscous effects in boundary layers, mixing processes, shock waves and heat transfer across temperature differences. In addition to a fresh approach to aerodynamic loss in turbomachinery, the paper provides an expert's review of work in many areas of gas path fluid mechanics for both axial and radial machines.

Using the Denton entropy generation approach to loss, O'Donnell and Davies[46] at the University of Limerick report the results of very detailed measurements of entropy generation in the suction side midspan boundary layer of a turbine blade mounted in a subsonic linear cascade at a Reynolds number of 1.85×10^5. They found that 75% of the

entropy generated by the boundary layer occurred within the laminar region (50% of the suction surface length). Conventional wisdom, based on considerations of aerodynamic drag, holds that turbulent boundary layer losses are significantly higher than laminar losses. The Limerick work shows that the reverse is true, with the greater portion of entropy being generated by the high shear forces found in the very thin, laminar midspan suction side boundary layer. One is led to speculate that such detailed measurements of entropy made in an endwall boundary layer might yield similar results, concerning laminar flow endwall contributions to secondary flow losses in turbine cascades.

CONCLUSIONS

Over the last 25 years, through the research efforts of many investigators, a sharper and more quantified picture of secondary flow in turbine airfoil cascades has emerged. In his review of the subject, Sieverding[1] called for the need to evaluate the significance of various aspects of the complex flow. Some progress in that evaluation has been reviewed here, from which one may conclude the following:

1) The basic secondary flow picture (e.g. Fig. 1) put forth by various teams of investigators in the 1970's has since been verified by a number of other studies.

2) More details of this basic picture have emerged or been proposed (e.g. Figs. 5 and 6). Detailed measurements of velocity and pressure are needed to quantify their significance.

3) A more complete understanding of the separation process of the inlet boundary layer (or more generally, the redistribution of the inlet vorticity) is needed. The flow parameter given in Equ. (1) is a first step in the direction of predicting properties of the separated flow.

4) Research into and development of geometries and devices to reduce or control secondary flow has made some progress. One recent investigation (the leading edge bulb in Fig. 8) is particularly promising. The apparently strong effect it has on losses points out the need for basic endwall flow measurements.

5) In the last twenty years the overall features of secondary flow have been successfully modeled by investigators using a variety of CFD codes. However, the lack of an adequate turbulence model seems to be one major cause of an inability to routinely predict endwall loss accurately. Denton[45] maintains that even for the straightforward problem of calculating the loss of a two-dimensional cascade, an *a priori* prediction using the best available methods, is unlikely to be accurate to better than about ± 20%. Endwall loss *a priori* CFD predictions are probably no more accurate than Denton's estimate.

6) The underlying mechanisms causing secondary flow losses are not yet fully understood. The approach of thinking of loss in terms of entropy generation proposed by Denton[45] may provide new ways of dealing with these important problems.

Lastly, the author would make a strong case for more basic experiments to study secondary flows, either with cascades or with experiments such as endwall-cylinder flows that capture some aspects of the endwall flow physics. It has been the author's experience that CFD follows the experimenter, not the other way around. It is with experiments that new flow features are found out. These new features can then be modeled by numerical codes or other analytical models.

ACKNOWLEDGEMENTS

The author thanks Laurie Hockla of the University of Connecticut and Sandor Becz of Pratt & Whitney, United Technologies Corporation for their help in preparing this paper.

REFERENCES

1. Sieverding, C.H. 1985. Recent Progress in the Understanding of Basic Aspects of Secondary Flows in Turbine Blade Passages. ASME Jour. of Turbomachinery. **107:** 248-257.
2. Bradshaw, P. 1996. Turbulence Modeling with Application to Turbomachinery. Prog. Aerospace Sci. **32:** 575-624.
3. Sharma, O.P., and Butler, T.L. 1987. Predictions of Endwall Losses and Secondary Flows in Axial Flow Turbine Cascades. ASME Jour. of Turbomachinery. **109:** 229-236.
4. Langston, L.S., Nice, M.L. and Hooper, R.M. 1977. Three-Dimensional Flow Within a Turbine Cascade Passage. ASME Jour. of Engineering for Power. **99:** 21-28.
5. Langston, L.S. 1980. Crossflows in a Turbine Cascade Passage. ASME Journal of Engineering for Power. **102:** 866-874.
6. Sieverding, C.H. and Van den Bosche. 1983. The Use of Colored Smoke to Visualize Secondary Flows in a Turbine-Blade Cascade. Jour. of Fluid Mechanics. **134:** 85-89.
7. Marchal, P.H. and Sieverding, C.H. 1977. Secondary Flows Within Turbomachinery Bladings. Secondary Flows in Turbomachines. AGARD CP No. 214. Paper No. 11.
8. Yamamoto, A. 1987. Production and Development of Secondary Flows and Losses in Two Types of Straight Turbine Cascades: Part I – A Stator Case. ASME J. of Turbo. **109:** 186-193.
9. Yamamoto, A. 1987. Production and Development of Secondary Flows and Losses in Two Types of Straight Turbine Cascades: Part 2 – A Rotor Case. ASME J. of Turbo. **109:** 194-200.
10. Gregory-Smith, D.G., Graves, C.P., and Walsh, J.A. 1988. Growth of Secondary Losses and Vorticity in an Axial Turbine Cascade. ASME Jour. of Turbomachinery. **110:** 1-8.
11. Harrison, S. 1990. Secondary Loss Generation in a Linear Cascade of High-Turning Turbine Blades. ASME Jour. of Turbomachinery. **112:** 618-624.
12. Goldstein, R.J. and Spores, R.A. 1988. Turbulent Transport on the Endwall in the Region Between Adjacent Turbine Blades. ASME Jour. of Heat Transfer. **110:** 862-869.
13. Wang, H.P., Olson, S.J., Goldstein, R.J. and Eckert, E.R.G. 1997. Flow Visualization in a Linear Turbine Cascade of High Performance Turbine Blades. ASME J. of Turbo. **119:** 1-8.
14. Baker, C.J. 1979. The Laminar Horseshoe Vortex. Jour. of Fluid Mechanics. **95:** 347-367.
15. Hodson, H.P. and Dominy, R.G. 1989. Three-Dimensional Flow in a Low-Pressure Turbine Cascade at Its Design Condition. ASME Jour. of Turbomachinery. **109:** 177-185.
16. Green, Sheldon I. 1995. *Fluid Vortices*. 1-9. Kluwer Academic Publishers.
17. Eckerle, W.A. and Langston, L.S. 1987. Horseshoe Vortex Formation Around a Cylinder. ASME Jour. of Turbomachinery. **109:** 278-285.
18. Moore, J. and Ransmayr, A. 1984. Flow in a Turbine Cascade: Part 1 – Losses and Leading Edge Effects. ASME Jour. of Engineering for Gas Turbines and Power. **106:** 400-408.
19. Ballio, F., Bettoni, C. and Franzetti, S. 1998. A Survey of Time-Averaged Characteristics of Laminar and Turbulent Horseshoe Vortices. ASME Jour. of Fluids Engineering. **120:** 233-242.
20. Eckerle, W.A. and Awad, J.K. 1991. Effect of Freestream Velocity on the Three-Dimensional Separated Flow Region in Front of a Cylinder. ASME Jour. of Fluids Engineering. **113:** 37-44.

21. Kang, M.B., Kohli, A. and Thole, K.A. 1999. Heat Transfer and Flowfield Measurements in the Leading Edge Region of a Stator Vane Endwall. ASME J. of Turbo. **121:** 558-568.
22. Harrison, S. 1992. The Influence of Blade Lean on Turbine Losses. ASME Jour. of Turbomachinery. **114:** 184-190.
23. Duden, A., Raab, I., Fottner, L. 1999. Controlling the Secondary Flow in a Turbine Cascade by Three-Dimensional Airfoil Design and Endwall Contouring. ASME J. of Turbo. **121:** 191-199.
24. Prümper, H. 1972. Application of Boundary Fences in Turbomachinery. AGARD AG No. 164. Paper No. II-3: 315-331.
25. Gallus, H.E. and Kummel, W. 1977. Secondary Flows and Annulus Wall Boundary Layers in Axial-Flow Compressor and Turbine Stages. AGARD CPP No. 214. Paper No. 4: 1-15.
26. Chung, J.T. and Simon, T.W. 1993. Effectiveness of the Gas Turbine Endwall Fences in Secondary Flow Control at Elevated Freestream Turbulence Levels. ASME Paper No. 93-GT-51.
27. Aunapu, Nicole V., Volino, Ralph J., Flack, Karen A. and Stoddard, Ryan M. 2000. Secondary Flow Measurements in a Turbine Passage with Endwall Modification. ASME No. 2000-GT-212.
28. Deich, M.E., Zaryanskin, A.E., Fillipov, G.A. and Zatsepin, M. 1960. Method of Increasing the Efficiency of Turbine Stages with Short Blades. *Teploenergetikia*. **2:** 240-254.
29. Morris, A.W.H. and Hoare, R.G. 1975. Secondary Loss Measurements in a Cascade of Turbine Blades with Meridional Wall Profiling. ASME Paper No. 75/GT-13.
30. Kopper, F.C. and Milano, R. 1981. Experimental Investigation of Endwall Profiling in a Turbine Vane Cascade. AIAA Journal. **19:** 1033-1040.
31. Dossena, V., Perdichizzi, A. and Savini, M. 1999. The Influence of Endwall Contouring on the Performance of a Turbine Nozzle Guide Vane. ASME Jour. of Turbomachinery. **121:** 200-208.
32. LaFleur, Ronald S., Whitten, Timothy S. and Aranjo, Juan A. 1999. Second Vane Endwall Heat Transfer Reduction by Iceform Contouring. ASME Paper No. 99-GT-422.
33. LaFleur, R.S. and Langston, L.S. 1993. Drag Reduction of a Cylinder/Endwall Junction Using the Iceformation Method. ASME Jour. of Fluids Engineering. 115: 26-32.
34. Sauer, H., Müller, R. and Vogeler, K. 2000. Reduction of Secondary Flow Losses in Turbine Cascades by Leading Edge Modifications at the Endwall. ASME paper No. 2000-GT-473.
35. Sauer, H. and Wolf, H. 1997. Influencing the Secondary Flow in Turbine Cascades by the Modification of the Blade Leading Edge. 2. European Conference of Turbomachinery. Antwerpen.
36. Hah, C. 1984. A Navier-Stokes Analysis of Three-Dimensional Turbulent Flows Inside Turbine Blade Rows at Design and Off-Design Conditions. ASME Jour. of Engineering for Gas Turbines and Power. **106:** 421-429.
37. Dorney, D.J. and Davis, R.L. 1992. Navier-Stokes Analysis of Turbine Blade Heat Transfer and Performance. ASME Jour. of Turbomachinery. **114:** 795-806.
38. Graziani, R.A., Blair, M.F., Taylor, J.R. and Mayle, R.E. 1980. An Experimental Study of Endwall and Airfoil Surface Heat Transfer in a Large Scale Turbine Blade Cascade. ASME Jour. of Engineering for Power. **102:** 257-267.
39. Hartland, J.C., Gregory-Smith, P.G., Harvey, N.W. and Rose, M.G. 2000. Nonaxisymmetric Turbine End Wall Design: Part II – Experimental Validation. ASME J. of Turbo. **122:** 286-293.
40. Gregory-Smith, D.G. and Cleak, J.G.E. 1992. Secondary Flow Measurements in a Turbine Cascade with High Inlet Turbulence. ASME Jour. of Turbomachinery. **114:** 173-183.
41. Harvey, Neil W., Rose, Martin G., Taylor, Mark D., Shahrokh, Hartland, Jonathan and Gregory-Smith, David G. 2000. Nonaxisymmetric Turbine End Wall Design: Part I – Three-Dimensional Linear Design System. ASME Jour. of Turbomachinery. **122:** 278-285.
42. Moore, H. and Gregory-Smith, D.G. 1996. Transition Effects on Secondary Flows in a Turbine Cascade. ASME Paper No. 96-GT-100.
43. Senoo, Y. 1958. The Boundary Layer on the End Wall of a Turbine Nozzle Cascade. Transactions of the ASME. **80:** 1711-1720.
44. Taylor, E.S. 1971. Boundary Layers, Wakes and Losses in Turbomachines. MIT Gas Turbine Report No. **105:** 1-3.
45. Denton, J.D. 1993. Loss Mechanisms in Turbomachines. ASME J. of Turbo. **115:** 621-650.
46. O'Donnell, F.K. and Davies, M.R.D. 2000. Turbine Blade Entropy Generation Rate Part II: The Measured Loss. ASME Paper No. 2000-GT-266.